Ion Current in Hall Thrusters

Ira Katz, Richard R. Hofer, and Dan M. Goebel, *Fellow, IEEE*

Abstract—To match the observed thrust and discharge current in Hall thrusters, computer simulations have typically assumed anomalous electron transport mechanisms, such as Bohm diffusion, to enhance electron mobility across magnetic field lines. Without enhanced electron transport, the simulations predict a much lower discharge current than observed, and too much of the potential drop is downstream of the channel exit. Rather than search for mechanisms to increase the electron scattering frequency, we seek to identify mechanisms that would increase the fraction of the current carried by ions, thus reducing the required electron current. We describe two mechanisms that enhance the current carried by ions. The first mechanism increases the ion current carried in the channel by simply including the effects of multiply charged ions on the plasma response. The importance of using accurate ionization cross sections and the need to include multiply charged ions even for discharge voltages of 300 V are discussed. The second mechanism is a process we term "ion reflux." In this process, current is carried by ions generated downstream of the channel exit. Portions of these ions impact the center of the thruster and are neutralized by cathode electrons. A large fraction of the resultant neutral atoms are reionized as they pass through the main exhaust beam. These newly born ions then carry additional current through the plume. Since neutrals freely move across magnetic field lines, ion reflux effectively enhances the cross-field electron transport. This second mechanism operates downstream of the exit plane and does not enhance electron transport in the acceleration region. Both of these mechanisms, i.e., multiply charged ions and ion reflux, reduce the need to invoke anomalous electron transport mechanisms in Hall thruster computer simulations. However, to date, no Hall thruster simulation has produced results in agreement with data without assuming some anomalous electron transport.

Index Terms—Electron transport, Hall thrusters, particle simulations, plasma propulsion.

I. INTRODUCTION

HALL thrusters are rapidly becoming the most widely accepted form of electric propulsion on communication satellites. Since the 1970s, more than 50 satellites with over 200 Hall thrusters have been flown [1]. However, there are still questions about the basic physical mechanisms that determine the electrical characteristics and performance of these thrusters. Computer simulations, such as HPHall-2 [2]–[4], that model Hall thruster plasma and erosion processes have been developed. These codes assume that, inside the channel,
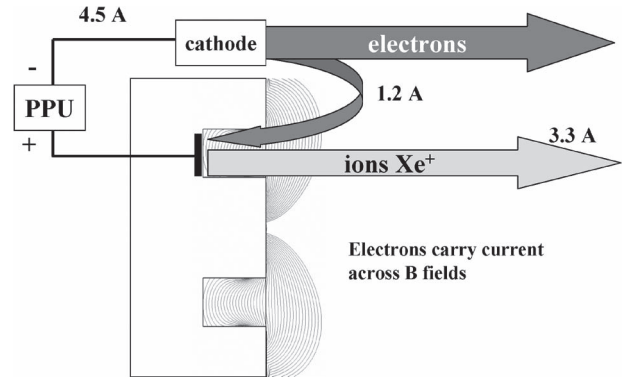
Fig. 1. Current flow in a typical Hall thruster simulation. About a quarter of the current in the channel is by electrons that originated in the hollow cathode.

about three quarters of the current is carried by beam ions and about one quarter is counter streaming electrons from the hollow cathode (Fig. 1). If the simulations only use classical electron scattering mechanisms, they predict much lower circuit currents and performance than measured. Simulations can be made to agree more closely with experimental data by invoking anomalous transport mechanisms, such as "Bohm diffusion" [5], to enhance electron transport across magnetic field lines.

In the past few years, research on electron transport mechanisms in the channel has focused on the interactions between the plasma and the channel walls [6]. Several advances have been made; in particular, the plasma has been forced to satisfy the Bohm sheath condition [7], and accurate formulations have been developed to model the transport due to secondary electron emission at the channel wall [8]. Other researchers have shown that the channel width is too short to develop high-amplitude scattering due to changes in the energy distribution caused by secondary electrons accelerated by the wall plasma sheath [9]. Other groups [10]–[12] have shown that, inside the channel, only a small fraction of Bohm diffusion is required to explain the cross-field electron transport, whereas outside the channel, anomalous scattering of the magnitude of Bohm diffusion is needed to obtain plasma potentials and densities that resemble the experimental measurements.

The low electron mobility calculated in Hall thrusters by the codes is expected. The magnetic fields in Hall thrusters are designed to reduce electron mobility so much that electrons move up the channel slower than the ions that are accelerated down the channel. As discussed above, most of the current in the channel is carried by the ions. The ions are massive enough that their trajectories are not significantly modified by the magnetic field, but the electrons are trapped on field lines until undergoing a scattering event. Rather than search for mechanisms to increase the electron scattering frequency, the objective of this paper is to identify mechanisms that
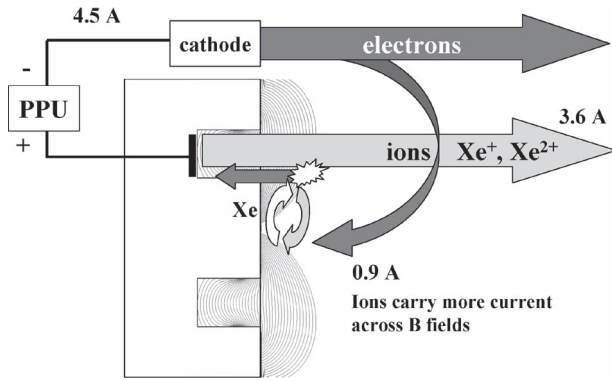
Fig. 2.   New concept of current flow in Hall thrusters with a greater fraction of the cross-field current carried by ions, including "ion reflux" near the thruster center line.

Fig. 3.   Geometry and grid used for plasma simulations with HPHall-2.

TABLE I
HPHALL-2 INPUTS FOR PLASMA SIMULATIONS

Discharge voltage (V)	300
Anode mass flow rate (mg/s)	5
Discharge chamber outer diameter (mm)	100
Discharge chamber width (mm)	15
Discharge chamber length (mm)	25
Simulation time step (s)	5×10^{-8}

would increase the fraction of the current carried by ions in the simulations, and thus reduce the required electron current. Increasing the ion current has great leverage, since, even in the present simulations, ions carry three times the channel current of electrons. A 1% increase in ion current would reduce the electron current by 3%.

Two mechanisms that increase the calculated ion current have been identified. The first increases the ion current carried in the channel by simply including the effects of doubly charged ions. The second is a process we term "ion reflux". In this process, current is carried by ions generated downstream of the channel exit. Portions of these ions impact the center of the thruster and are neutralized by cathode electrons. A large fraction of the resultant neutral atoms are reionized as they pass through the main exhaust beam. These newly born ions then carry additional current through the plume. Since neutrals freely move across magnetic field lines, ion reflux effectively enhances the cross-field electron transport. This new concept of current flow in Hall thrusters is shown in Fig. 2. This second mechanism operates downstream of the exit plane and does not enhance electron transport in the channel ion acceleration region.

The first mechanism has a simple basis. HPHall uses an *ad hoc* electron impact cross section for ionization from Xe^+ to Xe^{2+} that is much smaller than published cross sections from experiments. Calculations for the SPT-100 thruster that use the published cross sections are presented in the following sections. These calculations show that, even with the decrease of the effective Bohm coefficient to 0.028 in the channel region, the code shows an increase in the ion current by 8% and a reduction in the channel electron current by 25% for the same fixed total current condition. Including triply charged xenon would further reduce the channel electron current and possibly eliminate the need for enhanced electron scattering to be introduced.

The second mechanism is more difficult to implement in the present simulations. Presented in the following sections are "back of the envelope" non–self-consistent calculations that demonstrate the viability of the "ion reflux" mechanism in carrying current across thruster magnetic field lines. These are just two specific mechanisms that enable ions to carry more of the cross-field current. There may be more mechanisms revealed as this general concept is further pursued.
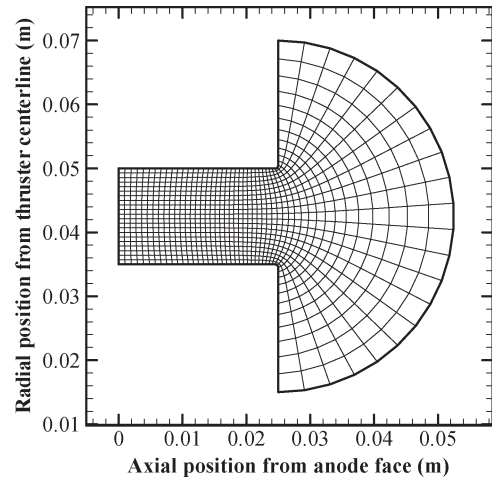
II. PLASMA SIMULATION PARAMETERS

Hall thruster plasma simulations were conducted with a modified version of HPHall-2. HPHall-2 is an axisymmetric quasi-neutral solver that employs a hybrid fluid/particle-in-cell (hybrid-PIC) numerical method to simulate the time-dependent evolution of the plasma inside the discharge chamber and near-field plume of a Hall thruster. HPHall, which was originally developed by Fife [2], was recently upgraded by Parra *et al.* [3], resulting in the HPHall-2 release. We have since performed further modifications of the code that have been documented in [4], [10], [13], and [14]. The results in this paper are based on the version described in [4].

The simulation results presented here are based on the SPT-100 geometry and magnetic field described in [10]. Fig. 3 shows the geometry and grid, and Table I presents some of the basic inputs used for the simulations.

III. DOUBLY-CHARGED IONS

A. Ionization Cross Section

For discharge voltages of 300 V or less, it is common practice in the literature to neglect the effects of multiply charged ion species on the plasma response. This approximation is usually justified based on experimental data, showing that the number flux fraction of doubly charged ions is about 6%–11% at this voltage [15], [16]. However, it has been observed that the fraction of multiply charged ion species increases with discharge voltage [17].

Our previous work using HPHall-2 ran the simulation with singly charged ions for SPT-100 geometries [10], [13], [14]. We have now activated the doubly charged ion species option
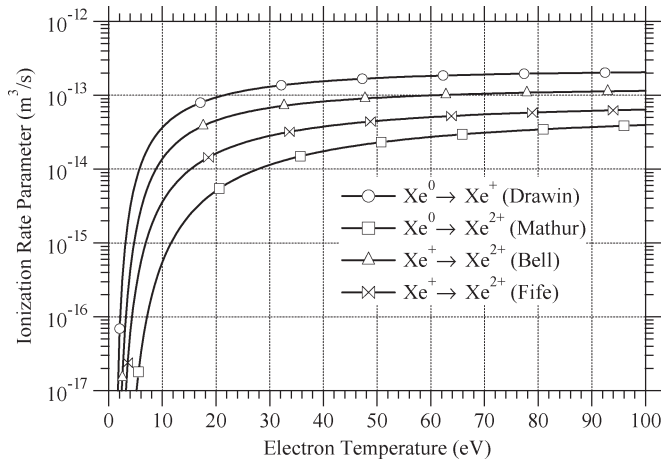
Fig. 4. Ionization rate parameter versus electron temperature. The Xe^+ ionization rate parameter of Fife [2] has been updated in HPHall-2 with the experimental data of Bell [18].

Fig. 5. Ratio of the Xe^+ ionization rate parameter based on measured cross sections from Bell [18] to the estimates made by Fife in the original version of HPHall [2]. Between 5–30 eV, Fife underestimates the ionization rate parameter by a factor of 2–6.

in HPHall-2 since our plasma and erosion modeling of the BPT-4000 Hall thruster requires discharge voltages of up to 400 V [4], and there is a need to model other high-voltage Hall thrusters.

However, after activating the doubly charged ion model, it was noticed that the ionization rate predicted by the code was very low. It turns out that, in the absence of finding experimental data in the literature, Fife made an "educated guess" [2] in the original version of HPHall for the ionization rate parameter of singly charged xenon ($Xe^+ \rightarrow Xe^{2+}$) that underestimated the ionization rate compared with the experimental data of Bell [18]. In HPHall, the ionization rates of singly and doubly charged ions are computed from

$$\dot{n}_i^+ = \alpha(T_e)^{0 \rightarrow 1+} n_0 n_e$$
$$\dot{n}_i^{2+} = \alpha(T_e)^{0 \rightarrow 2+} n_0 n_e + \alpha(T_e)^{1+ \rightarrow 2+} n_e n_i^+ \quad (1)$$

where n_0 is the neutral density, n_e is the plasma density, n_i^+ is the plasma density, and the terms $\alpha(T_e)^{0 \rightarrow 1+}$, $\alpha(T_e)^{0 \rightarrow 2+}$, and $\alpha(T_e)^{1+ \rightarrow 2+}$ are the ionization rate parameters for the creation of singly and doubly charged ions from neutrals and singly charged ions, respectively. Fig. 4 shows the rate parameters for each ionization channel as a function of electron temperature. Single ionization from the ground state is approximated according to the Drawin ionization model [19]. The double ionization from the ground state is based on the experimental data of Mathur and Badrinathan [20] and fits the Drawin ionization model [19]. Both ground state ionization channels are unchanged in the present results, and only the ionization of singly charged xenon is modified by replacing the ionization rate parameter of Fife [2] with that of Bell [18]. With this change, the ionization rate parameters for all of the ionization channels is in excellent agreement with data used in other Hall thruster models such as those used by Garrigues *et al.* [21].

Fig. 5 plots the ratio of the Xe^+ ionization rate parameters of Bell and Fife. For electron temperatures of 5–30 eV, which is the range of interest for 300-V Hall thruster discharges, Fife underestimates the ionization rate parameter by a factor of 2–6.
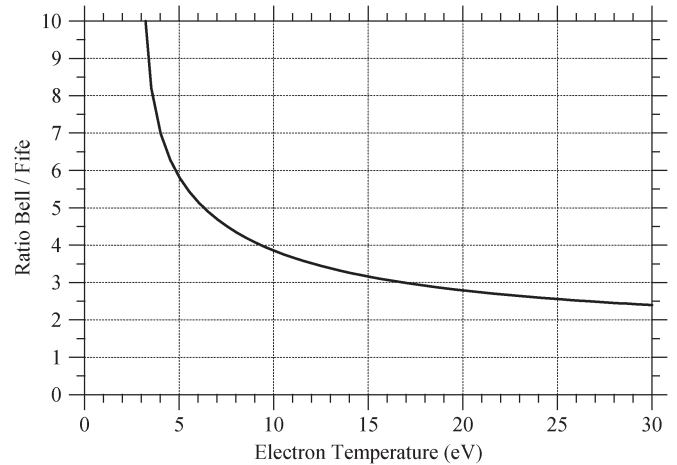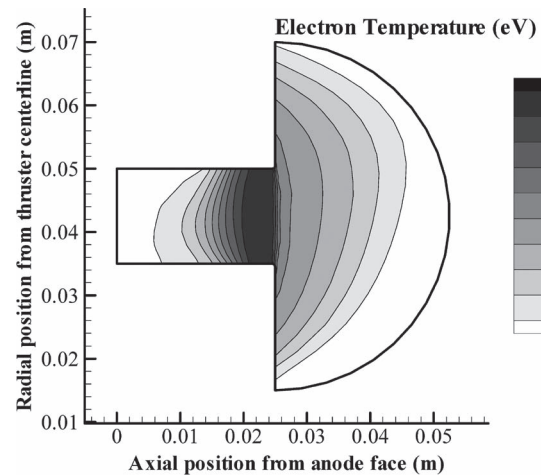

Fig. 6. Electron temperature distribution from HPHall-2 simulations using the updated ionization rate parameter for Xe^+.

The distribution of electron temperature from simulations using the updated ionization rate parameter for Xe^+ is shown in Fig. 6. The maximum electron temperature in Fig. 6 is 23 eV (or 8% of the discharge voltage), which is consistent with numerous Hall thruster experiments that have shown the maximum electron temperature to be in the range of 7%–14% of the discharge voltage [22]–[25]. The axial variation of electron temperature is also consistent with numerous experiments and simulations [23]–[29].

Table II lists maximum values from the simulation for the various particle densities and ionization rates after updating the Xe^+ ionization cross section. The maximum particle density of Xe^+ is about 30 times greater than Xe^{2+}. The maximum ionization rate, which is dominated by ground state ionization, is consistent with the SPT-100 simulations of Hagelaar *et al.* [26] that neglect doubly charged ions. With the Bell cross section, the maximum Xe^+ ionization rate is greater than the ground state double ionization rate by a factor of 2. Spatial differences in the discharge chamber of the particle densities and electron temperature act to cancel the roughly order of magnitude

TABLE II
MAXIMUM VALUES OF SEVERAL PLASMA PROPERTIES FROM
HPHALL-2 SIMULATIONS USING THE UPDATED IONIZATION
RATE PARAMETER FOR Xe$^+$

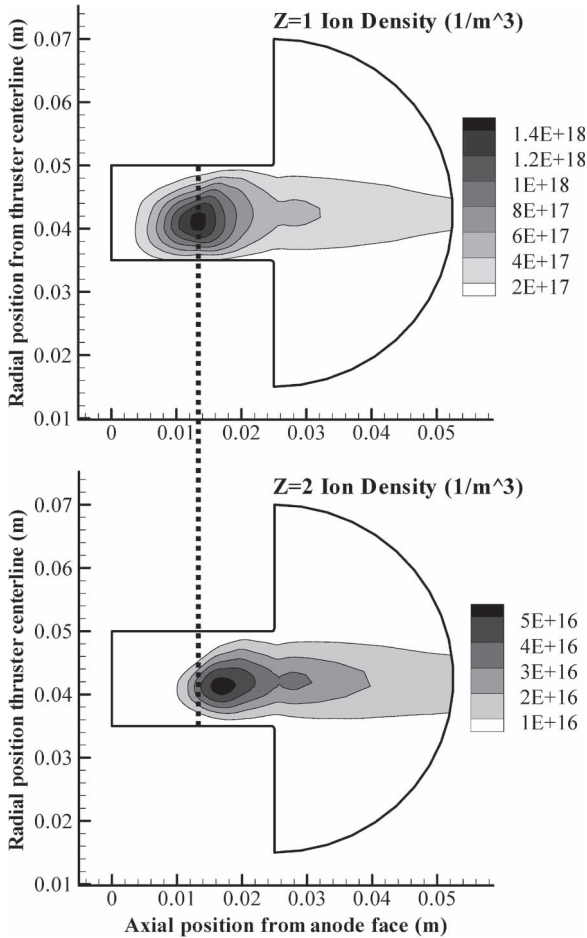|	
Plasma density (1/m^3)	1.6×10^{18}
Xe$^+$ density (1/m^3)	1.5×10^{18}
Xe^{2+} density (1/m^3)	5.0×10^{16}
Total ionization rate (1/m^3/s)	1.0×10^{24}
Xe$^0 \rightarrow$ Xe$^+$ ionization rate (1/m^3/s)	9.5×10^{23}
Xe$^+ \rightarrow$ Xe^{2+} ionization rate (1/m^3/s)	4.8×10^{22}
Xe$^0 \rightarrow$ Xe^{2+} ionization rate (1/m^3/s)	2.4×10^{22}

Fig. 7. Calculated (top) singly charged ion and (bottom) doubly charged ion densities. Doubly charged ions are created further downstream than singly charged ions, resulting in a larger divergence of the doubly charged ion plume. Note the difference in scale between the plots.

difference between the two ionization channels, yielding Xe^{2+} shown in Fig. 4.

Contours of the singly and doubly charged ion density are shown in Fig. 7 from simulations using the updated Xe$^+$ cross section. Due to their much smaller ionization cross section, the peak in the doubly charged ion density occurs about 4 mm further downstream than the singly charged ions. Being born further downstream increases the divergence of the doubly charged ion plume relative to the singly charged ion plume as the doubly charged ions are born in a region of higher radial electric fields and have a larger view factor out of the discharge chamber.
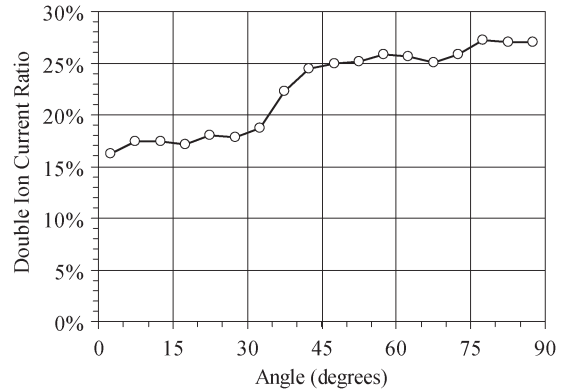

Fig. 8. Calculated ratio of doubly charged ion current to total ion current increasing away from the centerline. The plume-averaged doubly charged ion current fraction is 17%.

TABLE III
COMPARISON OF THE ION SPECIES FRACTIONS FROM HPHALL-2
SIMULATIONS WITH EXPERIMENT [15], [16]

Ion species	Kim [15]	King [16]	HPHall-2
Xe$^+$	0.930	0.888	0.911
Xe^{2+}	0.064	0.110	0.089
Xe^{3+}	0.006	0.002	0

The divergence of doubly charged ions is evident in Fig. 8, which plots the angular dependence of the doubly charged ion current fraction. Averaged over the entire plume, the doubly charged ion current fraction is 17%. The HPHall-2 calculation is consistent with experimental measurements from several Hall thruster models showing that the doubly charged ion plume is more divergent than the singly charged ion plume [15], [16], [30], [31].

As a check on the accuracy of the computed doubly charged ion species fraction, the current ratio within 5° of axis can be compared with the number flux ratios reported by Kim and King [15], [16]. The relationship between current ratio R and number flux ratio used in [15] and [16] is

$$\frac{f^{2+}}{f^+ + f^{2+}} = \frac{\frac{1}{2}j^{2+}}{j^+ + \frac{1}{2}j^{2+}}$$

$$R \equiv \frac{j^{2+}}{j^+ + j^{2+}}$$

$$j^{2+} = \frac{R}{1-R}j^+$$

$$\frac{f^{2+}}{f^+ + f^{2+}} = \frac{\frac{1}{2}R}{1-\frac{1}{2}R}. \tag{2}$$

The first data point plotted in Fig. 8 is the current ratio R for ions within 5° of the axis and has a value of

$$R_{\text{calc}} = 0.163 \Rightarrow \frac{f^{2+}}{f^+ + f^{2+}} = 0.089. \tag{3}$$

As shown in Table III, the calculated fraction of doubly charged ions is within the uncertainty of the experimental measurements.
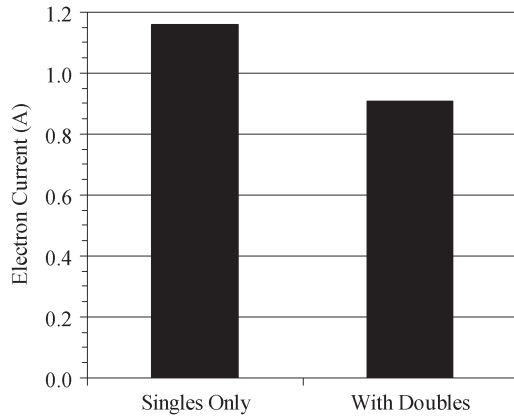
Fig. 9. Electron current in the channel is reduced by 25% after activating doubly charged ions in the simulation and using published ionization cross sections [18].

Fig. 10. Electron scattering frequency in the channel. The "Bohm" frequency is only 2.8% of the standard Bohm diffusion.

B. Current Balance

In this section, results are presented showing how including doubly charged ions in the simulation increases the predicted ion current in the channel while decreasing the need to invoke anomalous transport mechanisms needed to explain the experimentally observed discharge current (i.e., the sum of the ion and electron current).

The electron mobility perpendicular to magnetic field lines is given by

$$\mu_{e\perp} = \frac{e}{\nu_e m_e}\left(\frac{1}{1 + \Omega_e^2}\right) \qquad (4)$$

where ν_e is the electron collision frequency, Ω_e is the electron Hall parameter, and the rest of the symbols have their usual meaning. Wall collisions and turbulent plasma fluctuations are known to enhance the cross-field mobility in Hall thrusters. Including these effects can be accomplished by using a total effective electron collision frequency that is modeled as

$$\nu_e = \nu_{\text{eff}} \equiv \underbrace{\nu_{\text{en}} + \nu_{\text{ei}} + \nu_w}_{=\nu_c} + \nu_b \qquad (5)$$

where ν_{en} is the electron-neutral collision frequency, ν_{ei} is the electron–ion collision frequency, ν_w is the collision frequency of the electrons with the lateral walls, and ν_b is a collision frequency defined to capture the bulk effects of turbulent plasma fluctuations. The total "classical" collision frequency ν_c is defined here as the sum of the electron-neutral, electron–ion, and electron-wall collision frequencies. Further details of the electron mobility model are given in [4] and [10].

Updating the Xe^+ ionization rate significantly alters the predicted ion current in the channel. By implementing the published ionization rates of Xe^+, the calculated SPT-100 ion current inside the channel increases by approximately 8% (with respect to a model considering singly charged ions only at constant discharge current), decreasing the electron current needed to match the experimental discharge current by 25% (Fig. 9). Thus, neglecting doubly charged ions, even for discharge voltages of 300 V, can lead to nonnegligible errors in the calculated ion and electron currents.
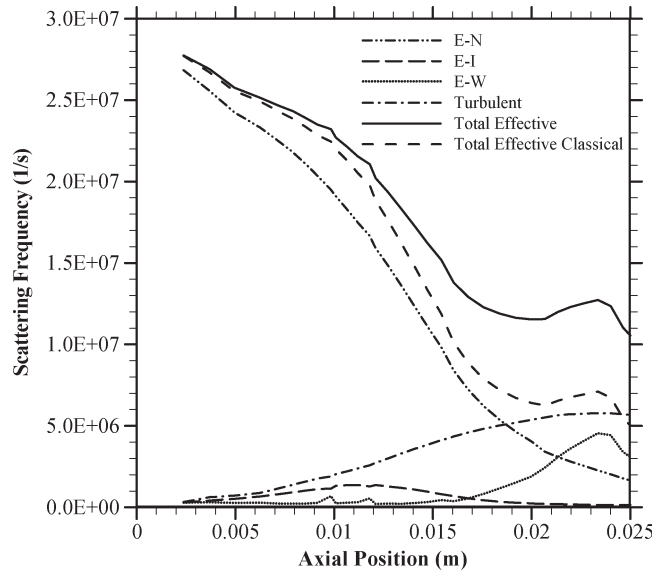
The electron scattering frequencies, averaged over magnetic field lines, as a function of axial position in the discharge chamber are shown in Fig. 10. The scattering frequency is dominated by the total classical scattering frequency over roughly two-thirds of the channel length. Only in the last third of the channel is the turbulent collision frequency needed to match the experimentally measured discharge current. In our model, the turbulent collision frequency is only 3.6% of Bohm diffusion for a model consisting of singly charged ions only. That is, for a turbulent collision frequency given by

$$\nu_b = \gamma \frac{1}{16}\omega_{\text{ce}} \qquad (6)$$

where ω_{ce} is the electron cyclotron frequency, and the parameter γ is equal to 0.036. When doubly charged ions are included in the simulation, allowing ions to carry more of the current, the turbulent collision frequency decreases to only 2.8% of Bohm diffusion. The net effect of implementing accurate higher ionization rates ($Xe^+ \rightarrow Xe^{2+}$, and in the future, $Xe^{2+} \rightarrow Xe^{3+}$) is to reduce or eliminate the need for anomalous electron transport within the channel.

IV. ION REFLUX

Downstream of the thruster exit plane, we propose that ions play a significant role in the current transport between the hollow cathode and the channel. Since they are born in a region of low electric potential, neutral gas atoms ionized downstream of the thruster exit are a source of low-energy ions. About half of these low-energy ions will drift toward the thruster centerline. These ions eventually impact the front of the thruster and are neutralized. Calculations presented below show that the resultant neutral atom has a high probability of being ionized before passing through the main beam, and will once again drift toward the centerline to be neutralized on the front of the thruster. This process, which we have termed "ion reflux," results in electrons being born in the beam by ionization (effectively enhancing the cross-field electron transport) and the
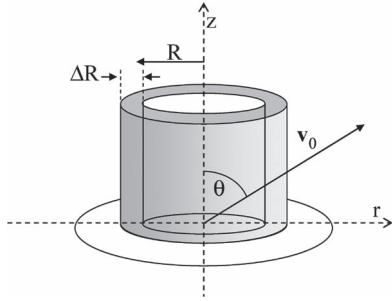
Fig. 11.   Trajectory of a neutral with velocity v_0 crossing through an ideal annular ion beam.

ions carrying the current across field lines and out of the beam. Some of the electrons from the hollow cathode go downstream where the magnetic field is weak and return along the axis to maintain charge balance on the thruster surface (Fig. 2). The rest of the hollow cathode electrons current neutralize the ion beam. The ion transport proposed here is similar to the cathode plasmas in low-pressure gas discharges [32]. This mechanism operates downstream of the exit plane and does not enhance electron transport in the acceleration region.

First, let us examine the case of an ideal thruster with a divergence-free beam. Assume that a xenon atom leaves the center insulator with a velocity v_0 and crosses through an ideal annular ion beam of mean radius R and thickness ΔR at angle θ, as shown in Fig. 11.

The transit time for a neutral atom to cross the annular beam is given by

$$\tau_{\text{transit}} = \frac{\Delta R}{v_0 \sin \theta}. \tag{7}$$

The ionization rate of neutrals is given by

$$\dot{n}_i = -\dot{n}_0 = n_0 n_e \alpha(T_e)^{0 \to 1+}. \tag{8}$$

The thruster plume is quasi-neutral, and we make the assumption that the slow ions generated have a density proportional to the beam ion density according to

$$n_e = n_{i,\text{tot}} = n_{i,\text{beam}} + n_{i,\text{slow}} = (1 + \beta) n_{i,\text{beam}}. \tag{9}$$

The beam ion density is given by

$$n_{i,\text{beam}} = \frac{I_{\text{beam}}}{2 \pi e R \Delta R v_{\text{beam}}}. \tag{10}$$

The neutral ionization time is given by

$$\tau_{\text{ionize}} = \frac{n_0}{\dot{n}_0} = -\frac{1}{n_e \alpha(T_e)^{0 \to 1+}}. \tag{11}$$

The probability that a neutral will transit the beam without being ionized is

$$P_{\text{escape}} = \exp\left(-\frac{\tau_{\text{transit}}}{\tau_{\text{ionize}}}\right)$$

$$\frac{\tau_{\text{transit}}}{\tau_{\text{ionize}}} = \frac{\Delta R}{v_0 \sin \theta} n_e \alpha(T_e)^{0 \to 1+}$$

$$\approx \frac{(1 + \beta) I_{\text{beam}} \alpha(T_e)^{0 \to 1+}}{2 \pi e R v_{\text{beam}} v_0 \sin \theta}. \tag{12}$$
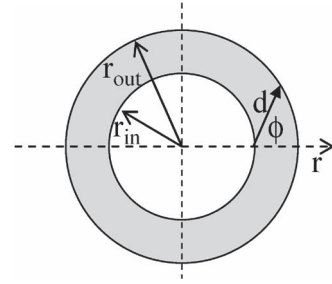

Fig. 12.   Projected path length d for a neutral crossing the channel at an angle ϕ to the local radius vector.

The probability of the neutral crossing the channel before being ionized is independent of the beamwidth because the transit time is linear in the width.

Putting in some representative numbers for isotropic emission and a neutral velocity corresponding to a central insulator surface temperature of 300 °C, we calculate that just over 1/4 of the neutrals would escape the annular beam before being ionized, e.g.,

$$v_{\text{beam}} \approx 2 \times 10^4 \text{ m/s}$$

$$v_0 \approx 300 \text{ m/s}$$

$$R = 0.0425 \text{ m}$$

$$\langle \sin \theta \rangle \approx 0.87$$

$$\beta \approx 1$$

$$I_{\text{beam}} = 3.6 \text{ A}$$

$$\langle z \rangle = R \langle \cos \theta \rangle \approx 0.5 \text{ R}$$

$$T_e(0.5 \text{ R}) \approx 10 \text{ eV}$$

$$\alpha(10 \text{ eV})^{0 \to 1+} \approx 4.16 \times 10^{-14} \text{ m}^{-3} \cdot \text{s}^{-1}$$

$$\frac{\tau_{\text{transit}}}{\tau_{\text{ionize}}} \approx 1.36$$

$$P_{\text{escape}} \approx 0.26. \tag{13}$$

The most uncertain inputs in (12) are the angle that goes into the transit time, the electron temperature, and the relative density of low-energy ions. We have also assumed that all neutrals are emitted from the middle of the central insulator. This assumption forces the projections of all neutral paths to be radial, which minimizes a particle path length across the channel. As shown in Fig. 12, if a neutral crosses the channel at projected angle ϕ with respect to the radial vector, the projected path length d will be larger than the channel width. The projected path length as a function of ϕ is given by

$$d = \Delta R \left(\sqrt{r_{\text{out}}^2 - r_{\text{in}}^2 \sin^2 \phi} - r_{\text{in}} \cos \phi \right) \tag{14}$$

where r_{in} and r_{out} are the inner and outer radii, respectively. While the maximum value of d is 2.4 ΔR, the typical values will be closer to ΔR. The density of low-energy ions is proportional to their production rate divided by their average velocity. While their production rate is much lower than the beam ion current, their velocity is also much lower than the beam ion

velocity, so to zeroth order, the low-energy density is the order of the ion beam density. The ionization rate was obtained by integrating the cross-sectional data of Mathur and Badrinathan [20] over a Maxwellian electron distribution. An increase in electron temperature to 15 eV reduces the escape probability by a factor of 3. Beam divergence increases the effective path lengths and also reduces the escape probability.

One of the results from the formulation above is an estimate of the neutral mean free path. To calculate the maximum neutral mean free path $\ell_{\max}$, we neglect the contribution of low-energy ions to the total plasma density ($\beta = 0$) as

$$
\begin{aligned}
\ell_{\max} &= v_0 \tau_{\mathrm{ionize}} \\
&= \frac{2\pi\, e\, R\, v_{\mathrm{beam}} v_0}{I_{\mathrm{beam}}\alpha(T_e)^{0\to1+}}\Delta R \\
&\approx 1.7\Delta R \\
&\approx 0.026 \text{ m}.
\end{aligned}
\tag{15}
$$

For the SPT-100, the maximum neutral mean free path is 26 mm, which is less than twice the channel width. The presence of low-energy ions will further reduce the mean free path.

To provide a quantitative estimate of the ion reflux current, calculations were performed on the probability that a neutral xenon atom would be ionized after leaving the insulator surface at the center of the thruster. In addition, the probability that the neutral would be ionized before reaching the ion beam density peak along its trajectory was calculated. The assumption is that since the potentials along the magnetic field lines follow the density, ions generated at radii smaller than the peak density would be accelerated back into the center by the potential gradient. These particles would eventually hit the insulator surface and recombine. Each ionization event inside the beam then generates an electron that contributes to the channel electron current.

Assume that half of the neutral gas escaping the channel has an inward radial velocity component and half is directed outward. If the channel ionization fraction is η, the ion current generated in the first transit equals the neutral gas flux times the ionization probability. Ions generated inside the radius of the density peak will eventually impact the center insulator. The resultant neutral gas is assumed to leave the surface with an isotropic cosine distribution. Those neutrals that were ionized in the first pass of neutrals from the center region then make up the second transit current. The fraction of these neutrals ionized inside the density peak, which, after being neutralized, impact the center insulator and are ionized on their way out, make up the third transit current. The resultant series can be summed to give the total "ion reflux" current.

To calculate the probability of a neutral being ionized, the beam plasma density was obtained from an Electric Propulsion Interactions Code (EPIC) [33] calculation of the SPT-100 (Fig. 13). For simplicity, it was assumed that all neutral xenon particles were emitted from the centerline of the downstream surface of the thruster with a thermal velocity corresponding to 300 °C, that the electron temperature in the plasma was a uniform 10 eV, and that the low-energy ions contribute about half the total density ($\beta = 1$). For each emission angle, both
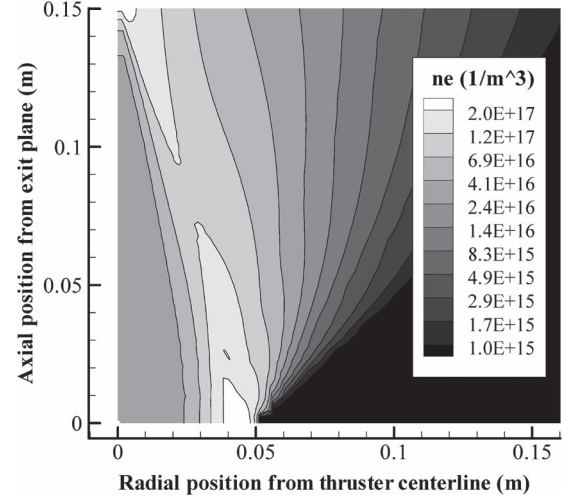

Fig. 13. SPT-100 plume density as calculated by the EPIC code used to estimate current due to ion reflux [33]. This density is only for primary beam ions and does not include any from low energy ions.

the total plasma column density N^∞ and the column density to the plasma peak N^p are calculated from

$$
\begin{aligned}
N^\infty &\equiv \int_0^\infty n_e(x)\,dx \\
N^p &\equiv \int_0^{\mathrm{peak}} n_e(x)\,dx.
\end{aligned}
\tag{16}
$$

The probability of a neutral being ionized is expressed in terms of the plasma column density along its path and is given by

$$
\begin{aligned}
\frac{dn_0}{dt} &= -\dot{n}_0 = -n_0\, n_e(x)\alpha(T_e)^{0\to1+} \\
\frac{dn_0}{dt} &= \frac{dn_0}{dx}\frac{dx}{dt} = v_0 \frac{dn_0}{dx} \\
\frac{1}{n_0}\frac{dn_0}{dx} &= -\frac{n_e(x)\alpha(T_e)^{0\to1+}}{v_0} \\
\ln\left(\frac{n_0(\infty)}{n_0(0)}\right) &= -\frac{\alpha(T_e)^{0\to1+}}{v_0}\int_0^\infty n_e(x)\,dx \\
N &\equiv \int_0^\infty n_e(x)\,dx \\
P_{\mathrm{ion}} &\equiv 1 - \frac{n_0(\infty)}{n_0(0)} \\
P_{\mathrm{ion}} &= 1 - \exp\left(-\frac{N\alpha(T_e)^{0\to1+}}{v_0}\right).
\end{aligned}
\tag{17}
$$

The ionization probabilities are averaged over the cosine of the angle with respect to the normal given by

$$
\begin{aligned}
P_{\mathrm{ion}}^\infty &= \left\langle 1 - \exp\left(-\frac{N^\infty\alpha(T_e)^{0\to1+}}{v_0}\right)\right\rangle_{\cos\theta} \\
P_{\mathrm{ion}}^{\mathrm{peak}} &= \left\langle 1 - \exp\left(-\frac{N^{\mathrm{peak}}\alpha(T_e)^{0\to1+}}{v_0}\right)\right\rangle_{\cos\theta}.
\end{aligned}
\tag{18}
$$

The loss rate of neutrals is proportional to the electron density, times the temperature-dependent ionization rate parameter $\alpha(T_e)^{0\to1+}$, divided by the neutral atom velocity. The ion current is estimated by assuming that all the neutrals leave the channel at the peak in the plasma density. Half leave the channel with positive radial velocities. The probability that these neutrals are ionized is approximately $P_{\text{ion}}^{\text{peak}}$. The probability that the other half of the neutrals with negative radial velocities will be ionized before they reach the next density peak is approximately P_{ion}^{∞}. These ions are transported to the center insulator by the local fields, where they recombine. The resultant neutrals have a probability of $P_{\text{ion}}^{\text{peak}}$ being ionized again before reaching the ion beam density peak. Those that are ionized before the peak are again transported back to the center insulator, where they are again reemitted as a neutral. When the neutral makes it past the beam density peak, it still has a finite probability $P_{\text{ion}}^{\infty} - P_{\text{ion}}^{\text{peak}}$ of being ionized, but will no longer be focused back to the center insulator. The total ion current generated by the neutral gas coming from the thruster is then given by

$$
\begin{aligned}
I_i &= e\dot{n}_i \\
&= (1-\eta)\frac{e\dot{m}}{m_{Xe}} \\
&\quad \times \left(\frac{1}{2}P_{\text{ion}}^{\text{peak}} + \frac{1}{2}P_{\text{ion}}^{\infty}\left(1 + P_{\text{ion}}^{\text{peak}}\left(1 + P_{\text{ion}}^{\text{peak}}(1+\cdots)\right)\right)\right. \\
&\quad \left. + \frac{1}{2}\left(P_{\text{ion}}^{\infty} - P_{\text{ion}}^{\text{peak}}\right)\right) \\
&= (1-\eta)\frac{e\dot{m}}{m_{Xe}} \\
&\quad \times \left(\frac{1}{2}P_{\text{ion}}^{\text{peak}} + \frac{1}{2}P_{\text{ion}}^{\infty}\frac{1}{1-P_{\text{ion}}^{\text{peak}}} + \frac{1}{2}\left(P_{\text{ion}}^{\infty} - P_{\text{ion}}^{\text{peak}}\right)\right)
\end{aligned}
$$

$$
I_i = (1-\eta)\frac{e\dot{m}}{m_{Xe}}\frac{1}{2}P_{\text{ion}}^{\infty}\left(1 + \frac{1}{1-P_{\text{ion}}^{\text{peak}}}\right). \tag{19}
$$

Propellant utilization and the ion current are from the SPT-100 calculation presented in Section III, i.e.,

$$
\eta = 0.9
$$
$$
\frac{e\dot{m}}{m_{Xe}} = 3.65 \text{ A}
$$
$$
P_{\text{ion}}^{\infty} = 0.85
$$
$$
P_{\text{ion}}^{\text{peak}} = 0.59
$$
$$
I_i = (1-\eta)\frac{e\dot{m}}{m_{Xe}}\frac{1}{2}P_{\text{ion}}^{\infty}\left(1 + \frac{1}{1-P_{\text{ion}}^{\text{peak}}}\right)
$$
$$
I_i = 0.4 \text{ A}. \tag{20}
$$

This estimate suggests that the ion reflux mechanism could supply 0.4 A of electrons into the beam, about half the 0.9 A of electrons in the HPHall-2 calculation. While this is just an estimate, and there are certainly some electrons that directly go from the hollow cathode into the channel, this simple

TABLE IV
TOTAL ION CURRENT AT DIFFERENT DISTANCES FROM THE SPT-100
EXIT PLANE IN THE VERY NEAR FIELD (FROM KIM [34])

Axial Position (mm)	Total Ion Current (A)
10	3.97
25	4.92
50	4.95
100	4.51
200	3.86

calculation shows that ion transport downstream of the channel exit may play an important role in transporting electrons across field lines and completing the circuit.

There is experimental evidence to support this magnitude of low-energy ions just downstream of the exit plane. Kim [34] used an upstream-facing Faraday probe to measure the ion current in the near plume of an SPT-100 thruster operating at the same conditions used in the aforementioned analysis. He found a marked increase in the total ion current between 10 and 25 mm downstream of the exit plane, as shown in Table IV. The location and magnitude of the ion-measured current increase is consistent with the presented results. Similar results were reported by Hofer and Gallimore on a 5-kW Hall thruster [35]. Prioul *et al.* [36] has also published SPT-100 data showing intense line emission from Xe^{+} along the axis just downstream of the exit plane, consistent with the ion reflux picture that low-energy ions would be focused into that area.

V. CONCLUSION

Two mechanisms, i.e., ion current from multiply charged ions in the thruster channel and "ion reflux" downstream in the near-field plume, that increase the fraction of current carried across magnetic field lines by ions and reduce the need to invoke anomalous electron transport in Hall thruster simulations have been presented. Since the electron current in the channel is less than a third of the ion current, small percentage increases in the current carried by ions lead to large fractional decreases in the electron current. With respect to multiply charged ions, the major contribution of this paper is to point out the importance of using accurate ionization cross sections and the need to include multiply charged ions even for 300-V discharge voltages.

The importance of the second mechanism (i.e., "ion reflux") is supported by numerical estimates and remains to be validated with 2-D self-consistent calculations and laboratory measurements. However, the presented estimates show that ions can play a significant role in closing the circuit between the hollow cathode and the thruster channel. Ions play a similar role near the cathode plasma in low-pressure gas discharges, so the presence of this mechanism in Hall thrusters should not be considered unreasonable. Since ions and neutrals are not magnetized, unlike the electrons, they easily move between the channel and the center insulating surface, providing current transport that may reduce the need for anomalous electron transport mechanisms to be invoked. However, the impact of ion reflux on electron mobility very strongly depends on where the ionization occurs. If it is very close to the channel exit plane, in a region of strong electric fields, the classical

electron mobility may be high enough to carry the current. If the bulk of the ions are generated significantly downstream, the classical mobility will be far too low to account for the observed anode currents. This question can only be answered with self-consistent multidimensional models and laboratory experiments. This mechanism operates downstream of the exit plane and does not enhance electron transport in the acceleration region.

The presented calculations show the importance of using accurate models of the classical processes in Hall thruster simulations. Only by using very accurate models of classical processes can the magnitude of anomalous transport mechanisms be determined. The need for accurate classical models extends well beyond ionization cross sections and also includes, for example, wall sheath interactions and neutral atom transport. It is anticipated that improved models will eventually enable Hall thruster simulations that are truly predictive and that fully describe the thruster physics. However, to date, no Hall thruster simulation has produced results in agreement with data without assuming some anomalous electron transport.

REFERENCES

[1] T. M. Randolph, "Qualification of commercial electric propulsion systems for deep space missions," presented at the 30th Int. Propulsion Conf., Florence, Italy, Sep. 17–20, 2007, IEPC Paper 2007-271.

[2] J. M. Fife, "Hybrid-PIC modeling and electrostatic probe survey of Hall thrusters," Ph.D. dissertation, Aeronaut. Astronaut., Massachusetts Inst. Technol., Cambridge, MA, 1998.

[3] F. I. Parra, E. Ahedo, J. M. Fife, and M. Martinez-Sanchez, "A two-dimensional hybrid model of the Hall thruster discharge," *J. Appl. Phys.*, vol. 100, no. 2, pp. 023 304-1–023 304-11, 2006.

[4] R. R. Hofer, I. G. Mikellides, I. Katz, and D. M. Goebel, "BPT-4000 Hall thruster discharge chamber erosion model comparison with qualification life test data," presented at the 30th Int. Electric Propulsion Conf., Florence, Italy, Sep. 17–20, 2007, IEPC Paper 2007-267.

[5] D. Bohm, E. H. S. Burhop, and H. S. W. Massey, "The use of probes for plasma exploration in strong magnetic fields," in *The Characteristics of Electrical Discharges in Magnetic Fields*, 1st ed. A. Guthrie and R. K. Wakerling, Eds. New York: McGraw-Hill, 1949.

[6] E. Ahedo, "Radial macroscopic model of a plasma flowing along annular dielectric walls," *Phys. Plasmas*, vol. 9, no. 7, pp. 3178–3186, 2002.

[7] F. I. Parra and E. Ahedo, "Fulfillment of the Bohm condition on the HPHall fluid-PIC code," presented at the 40th AIAA/ASME/SAE/ASEE Joint Propulsion Conf., Fort Lauderdale, FL, Jul. 11–14, 2004, AIAA Paper 2004-3955.

[8] E. Ahedo, J. M. Gallardo, and M. Martinez-Sanchez, "Effects of the radial plasma–wall interaction on the Hall thruster discharge," *Phys. Plasmas*, vol. 10, no. 8, pp. 3397–3409, 2003.

[9] D. Sydorenko, A. Smolyakov, I. Kaganovich, and Y. Raitses, "Effects of non-Maxwellian electron velocity distribution function on two-stream instability in low-pressure discharges," *Phys. Plasmas*, vol. 14, no. 1, pp. 013 508.1–013 508.8, 2007.

[10] R. R. Hofer, I. G. Mikellides, I. Katz, and D. M. Goebel, "Wall sheath and electron mobility modeling in Hybrid-PIC Hall thruster simulations," presented at the 43rd AIAA/ASME/SAE/ASEE Joint Propulsion Conf. Exhibit, Cincinnati, OH, Jul. 9–11, 2007, AIAA Paper 2007-5267.

[11] G. J. M. Hagelaar, J. Bareilles, L. Garrigues, and J.-P. Bouef, "Role of anomalous electron transport in a stationary plasma thruster simulation," *J. Appl. Phys.*, vol. 93, no. 1, pp. 67–75, Jan. 2003.

[12] J. W. Koo and I. D. Boyd, "Modeling of anomalous electron mobility in Hall thrusters," *Phys. Plasmas*, vol. 13, no. 3, p. 033 501, Mar. 2006.

[13] M. Gamero-Castano and I. Katz, "Estimation of hall thruster erosion using HPHall," presented at the 29th Int. Electric Propulsion Conf., Princeton, NJ, Oct. 31–Nov. 4, 2005, IEPC Paper 2005-303.

[14] R. R. Hofer, I. Katz, I. G. Mikellides, and M. Gamero-Castano, "Heavy particle velocity and electron mobility modeling in hybrid-PIC hall thruster simulations," presented at the 42nd AIAA/ASME/SAE/ASEE Joint Propulsion Conf., Sacramento, CA, Jul. 9–12, 2006, AIAA Paper 2006-4658.

[15] S.-W. Kim and A. D. Gallimore, "Plume study of a 1.35-kW SPT-100 using an ExB probe," *J. Spacecr. Rockets*, vol. 39, no. 6, pp. 904–909, Nov./Dec. 2002.

[16] L. B. King and A. D. Gallimore, "Mass spectral measurements in the plume of an SPT-100 Hall thruster," *J. Propuls. Power*, vol. 16, no. 6, pp. 1086–1092, Nov./Dec. 2000.

[17] R. R. Hofer and A. D. Gallimore, "High-specific impulse hall thrusters, Part 2: Efficiency analysis," *J. Propuls. Power*, vol. 22, no. 4, pp. 732–740, Jul./Aug. 2006.

[18] E. W. Bell, N. Djuric, and G. H. Dunn, "Electron-impact ionization of In+ and Xe+," *Phys. Rev. A, Gen. Phys.*, vol. 48, no. 6, pp. 4286–4291, Dec. 1993.

[19] M. Mitchner and C. H. Kruger, *Partially Ionized Gases*. New York: Wiley, 1973.

[20] D. Mathur and C. Badrinathan, "Ionization of xenon by electrons—Partial cross sections for single, double, and triple ionization," *Phys. Rev. A, Gen. Phys.*, vol. 35, no. 3, pp. 1033–1042, Feb. 1987.

[21] L. Garrigues, I. D. Boyd, and J. P. Boeuf, "Computation of Hall thruster performance," *J. Propuls. Power*, vol. 17, no. 4, p. 772, 2001.

[22] D. Staack, Y. Raitses, and N. J. Fisch, "Temperature gradient in Hall thrusters," *Appl. Phys. Lett.*, vol. 84, no. 16, pp. 3028–3030, Apr. 2004.

[23] V. Kim, D. Grdlichko, V. Kozlov, A. Lazourenko, G. Popov, and A. Skrylnikov, "Local plasma parameter measurements by nearwall probes inside the SPT accelerating channel under thruster operation with Kr," presented at the 38th Joint Propulsion Conf., Indianapolis, IN, Jul. 7–10, 2002, AIAA Paper 2002-4108.

[24] J. M. Haas and A. D. Gallimore, "Considerations on the role of the Hall current in a laboratory-model thruster," *IEEE Trans. Plasma Sci.*, vol. 30, no. 2, pp. 687–697, Apr. 2002.

[25] J. A. Linnell and A. D. Gallimore, "Internal plasma potential measurements of a Hall thruster using plasma lens focusing," *Phys. Plasmas*, vol. 13, no. 10, pp. 103 504.1–103 504.9, 2006.

[26] G. J. M. Hagelaar, J. Bareilles, L. Garrigues, and J. P. Boeuf, "Two-dimensional model of a stationary plasma thruster," *J. Appl. Phys.*, vol. 91, no. 9, pp. 5592–5598, May 2002.

[27] N. B. Meezan, W. A. Hargus, and M. A. Cappelli, "Anomalous electron mobility in a coaxial Hall discharge plasma," *Phys. Rev. E, Stat. Phys. Plasmas Fluids Relat. Interdiscip. Top.*, vol. 63, no. 2, p. 026 410, Feb. 2001.

[28] Y. Raitses, D. Staack, A. Smirnov, and N. J. Fisch, "Space charge saturated sheath regime and electron temperature saturation in Hall thrusters," *Phys. Plasmas*, vol. 12, no. 7, p. 073 507, Jul. 2005.

[29] N. Dorval, J. Bonnet, J. P. Marque, E. Rosencher, S. Chable, F. Rogier, and P. Lasgorceix, "Determination of the ionization and acceleration zones in a stationary plasma thruster by optical spectroscopy study: Experiments and model," *J. Appl. Phys.*, vol. 91, no. 8, pp. 4811–4817, Apr. 2002.

[30] F. S. Gulczinksi and A. D. Gallimore, "Near-field ion energy and species measurements of a 5-kW Hall thruster," *J. Propuls. Power*, vol. 17, no. 2, pp. 418–427, Mar./Apr. 2001.

[31] J. E. Pollard, K. D. Diamant, V. Khayms, L. Werthman, D. Q. King, and K. H. De Grys, "Ion flux, energy, and charge-state measurements for the BPT-4000 Hall thruster," presented at the 37th AIAA/ASME/SAE/ASEE Joint Propulsion Conf. Exhibit, Salt Lake City, UT, Jul. 8–11, 2001, AIAA Paper 2001-3351.

[32] G. G. Lister, "Low-pressure gas discharge modelling," *J. Phys. D, Appl. Phys.*, vol. 25, no. 12, pp. 1649–1680, Dec. 1992.

[33] I. G. Mikellides, G. A. Jongeward, I. Katz, and D. M. Manzella, "Plume modeling of stationary plasma thrusters and interactions with the Express-A spacecraft," *J. Spacecr. Rockets*, vol. 39, no. 6, pp. 894–903, 2002.

[34] S. W. Kim, "Experimental investigations of plasma parameters and species-dependent ion energy distribution in the plasma exhaust plume of a Hall thruster," Ph.D. dissertation, Aerosp. Eng., Univ. Michigan, Ann Arbor, 1999.

[35] R. R. Hofer and A. D. Gallimore, "Recent results from internal and very-near-field plasma diagnostics of a high specific impulse Hall thruster," presented at the 28th Int. Electric Propulsion Conf., Toulouse, France, Mar. 17–21, 2003, IEPC Paper 2003-037.

[36] M. Prioul, A. Bouchoule, S. Roche, L. Magne, D. Pagnon, M. Touzeau, and P. Lasgorceix, "Insights on physics of Hall thrusters through fast current interruptions and discharge transients," presented at the 27th Int. Electric Propulsion Conf., Pasadena, CA, Oct. 15–19, 2001, IEPC Paper 2001-059.

Ira Katz received the B.S. degree in physical chemistry from Case Institute of Technology, Cleveland, OH, in 1967 and the Ph.D. degree in chemical physics from the University of Chicago, Chicago, IL, in 1971.

He was previously a Senior Vice President with S-Cubed Division, Maxwell Technologies, where he led investigations in spacecraft–plasma interactions and electric-propulsion-generated plasmas. He is currently the Supervisor of the Electric Propulsion Group, Jet Propulsion Laboratory (JPL), California Institute of Technology, Pasadena, CA, where he is responsible for electric propulsion systems in JPL's space science missions. He is a recognized leader in computer models of ion thruster physics and spacecraft charging, and has authored over 70 peer reviewed articles and almost a hundred conference publications.

Richard R. Hofer received the B.S.E. degree in mechanical engineering in 1998, and the B.S.E., M.S.E, and Ph.D. degrees in aerospace engineering from the University of Michigan, Ann Arbor, in 1998, 2000, and 2004, respectively.

He was previously a Research Scientist with the QSS Group, Inc., NASA Glenn Research Center, Cleveland, OH, where he designed several Hall thrusters ranging in power from 1 to 100 kW and specific impulses of 1000 to 4000 s. He is currently a member of the Technical Staff with the Jet Propulsion Laboratory, California Institute of Technology, Pasadena, CA, where he is responsible for the development of high-performance Hall thrusters and the validation of Hall thruster plasma and erosion models for deep space missions and plasma diagnostics. He has authored over 30 technical publications in the field of electric propulsion.

Dr. Hofer is a Senior Member of the American Institute of Aeronautics and Astronautics (AIAA), a member of the AIAA Electric Propulsion Technical Committee, and a member of the Joint Army Navy NASA Air Force (JANNAF) Electric Propulsion Panel.

Dan M. Goebel (M'93–SM'96–F'99) received the B.S. degree in physics, the M.S. degree in electrical engineering, and the Ph.D. degree in applied plasma physics from the University of California, Los Angeles, in 1977, 1978, and 1981, respectively.

He was previously a Research Scientist with HRL Laboratories, Malibu, CA, and a Principal Scientist with Boeing Electron Dynamic Devices (EDD), Torrance, CA, where he was the Supervisor of the Advanced Technology Group for microwave tube development and the Lead Scientist of the XIPS ion thruster program for commercial satellite station keeping. He is currently a Senior Research Scientist with the Jet Propulsion Laboratory, California Institute of Technology, Pasadena, CA, where he is responsible for the development of high-efficiency ion thrusters, advanced long-life components such as cathodes and grids, and thruster life model validation for deep-space missions. He is a recognized expert in advanced plasma and ion sources, microwave sources, high-voltage engineering, and pulsed-power switches. He is the author of over 100 technical papers, one book entitled *Fundamentals of Electric Propulsion: Ion and Hall Thrusters* to be published this year, and is the holder of 42 patents.

Dr. Goebel is the Chair of the American Institute of Aeronautics and Astronautics (AIAA) Electric Propulsion Technical Committee, Chair of the IEEE Electron Devices Society (EDS) Technical Committee on Vacuum Devices, member of the IEEE EDS Publications Committee, and Life Member of the APS and Sigma Xi. In 2004, he received the William Dunbar High Voltage Research Achievement Award.